Journal of Agricultural Engineering
https://www.agroengineering.org/

Design and experiment of a self-propelled target spraying machine for walnut orchards based on infrared laser sensing

Peng Yan,[1] Liangqing Li,[1] Kui Liu,[2] Lina Ma,[1] Wangyuan Zong,[1] Chengming Luo,[1] Yangjie Xu[1]

[1]College of Engineering, Huazhong Agricultural University, Wuhan, Hubei
[2]Agricultural Mechanization Research Institute, Xinjiang Academy of Agricultural Sciences, Urumchi, Xinjiang, China

Corresponding author: Chengming Luo, College of Engineering, Huazhong Agricultural University, Wuhan 430070, Hubei. China. E-mail: chmluo@mail.hzau.edu.cn

Please cite this article as doi: 10.4081/jae.2025.1775

Submitted: 15 March 2025
Accepted: 2 September 2025

Design and experiment of a self-propelled target spraying machine for walnut orchards based on infrared laser sensing

Peng Yan,[1] Liangqing Li,[1] Kui Liu,[2] Lina Ma,[1] Wangyuan Zong,[1] Chengming Luo,[1] Yangjie Xu[1]

[1]College of Engineering, Huazhong Agricultural University, Wuhan, Hubei
[2]Agricultural Mechanization Research Institute, Xinjiang Academy of Agricultural Sciences, Urumchi, Xinjiang, China

Corresponding author: Chengming Luo, College of Engineering, Huazhong Agricultural University, Wuhan 430070, Hubei. China. E-mail: chmluo@mail.hzau.edu.cn

Contributions: all authors made a substantive intellectual contribution, read and approved the final version of the manuscript and agreed to be accountable for all aspects of the work.

Conflict of interest: the authors declare no competing interests, and all authors confirm accuracy.

Availability of data and materials: All data generated or analyzed during this study are included in this published article.

Acknowledgements: this work was financially supported by Agriculture Mechanization Institute of Xinjiang Academy of Agricultural Sciences. The authors would like to thank Yengierik Village in Loq Township, Yecheng County for providing the walnut plantation for experiments.

Abstract

Spraying is an important operation for walnut orchards. To solve the problems of serious liquid waste, low operation efficiency and efficacy, high labor intensity and risk of health impact that existed in current spraying operations in walnut orchards in Xinjiang, a self-propelled target spraying machine was designed, fabricated and tested. Using the method of infrared laser ranging, the walnut tree canopies were detected and an automatic target spraying control system was developed. The structure, operation principle and design of key components of the machine were introduced. To improve the spraying accuracy, an operating speed-based time delay control strategy was designed and implemented. Field experiments showed that compared with continuous spraying, target spraying could save liquid consumption by 22.0%, 24.1% and 26.1% when the operating speeds were 0.4 m/s, 0.7 m/s and 1.0 m/s, respectively. The droplet deposition amounts at all seven sampling points reduced as the machine's operating speed increased and the orifice diameter of the nozzles decreased. However, the sprayed liquid was able to cover the whole canopy region of the walnut trees under all speed and orifice diameter combinations. When the operating speed varied, the delay distances for nozzle opening and nozzle closing were kept stable, with average values being 0.135 m and 0.184 m respectively, which indicates that the operating speed-based time delay control strategy was effective.

Key words: walnut orchard; target spraying; infrared laser ranging; solenoid valve; time delay.

Introduction

Walnut is a nutritious tree nut cultivated all over the world. As the world leader in walnut production, China yielded 5.935 million tons in 2022 (National Forestry and Grassland Administration, 2022). Xinjiang is one of the earliest and largest walnut planting regions in China because of its unique geographic and climatic advantages. To achieve high walnut yields, prevention and control of pests and diseases is the key. At present, chemical spraying is still the main means of walnut orchard management in Xinjiang. According to statistics, chemical spraying can reduce 66~90% walnut yield loss every year (Zheng *et al*., 2020; Li *et al*., 2023). Due to the low level of orchard standardization and differences in planting agronomy over the country, the development of automatic and intelligent spraying equipment in China is still slow. Currently, the commonly used spraying equipment in walnut orchards in Xinjiang are backpack sprayers and handheld high-pressure spray guns, which perform traditional continuous spraying. For walnut orchards with dense canopies and large tree gaps, continuous spraying causes serious chemical waste, low operation efficiency and efficacy, as well as high risk of worker poisoning (Chen *et al*., 2022; Chi *et al*., 2010).

To overcome the shortcomings of traditional spraying methods in orchards, variable-rate spraying technology was proposed and researched worldwide (Wei *et al*., 2022; Dou *et al*., 2022; Berk *et al*., 2016). The principle relies in locating and determining the main parameters of spraying targets (canopy volume, tree height, leaf area etc.) by appropriate sensors and spraying the desired amount of liquid to the target region (Yan *et al*., 2021; Gu *et al*., 2020; Zheng *et al*., 2020; Zhai *et al*., 2018). Over the past two decades, researchers have carried out a number of studies on variable spraying in orchards based on various types of sensors including infrared (Deng *et al*., 2008), ultrasonic (Gil *et al*., 2013; Jiang *et al*., 2016), laser (Li *et al*., 2018; Liu *et al*., 2018; Chen *et al*., 2023) and LiDAR (Mahmud *et al*., 2021; Dou *et al*., 2022).

Currently, variable-rate spraying based on optical and ultrasonic sensors is quite mature, and a number of commercialized products are available on the market. Precision spraying based on LiDAR technology is under development, and a big challenge for it is its high cost. Since Xinjiang's walnut orchards feature large row spacing and tree gaps, the adaptability of the readily available spraying products is undesirable. In this work, a self-propelled target spraying machine based on infrared laser detection and solenoid valve control was designed, developed and experimented. The key structural dimensions of the tracked chassis and working parameters of the air-assisted sprayer were determined according to the environmental conditions of the targeted walnut orchard. The machine structure and its working principle were introduced. After that, the design of the automatic spraying system, including its key components and the control hardware and program, were detailed.

The specific research objectives of this work include i) to provide a low-cost solution for target spraying of walnut orchards in Xinjiang, ii) to evaluate the operation performance of the designed target spraying machine in practical experiments, and iii) to determine the influence of different operation speeds on the control accuracy of the automatic spraying system.

Machine structure and working principle

Machine structure

Before designing the structure of the spraying machine, an investigation of the walnut orchard environment in Yecheng County, Kashgar, Xinjiang was conducted. It was found that the orchard surface was uneven with sandy soil and grasses, the row spacing was roughly 8 m and the distance between two trees along each row was about 5 m. The trees had an average height of 5 m, a canopy thickness of about 4 m, and an average trunk height of 1.5 m.

To adapt to the orchard conditions and tree dimensions, a self-propelled spraying machine based on a rubber-track chassis and an air-assisted sprayer was designed and manufactured. The chassis was driven by brushless DC motors (model: JJDM-48-1800, Jujie Co., Ltd.) for the purpose of facilitating remote control. The schematic diagram and a physical prototype of the machine are shown in Figure 1. Its main components included a tracked chassis, brushless DC motors, a battery pack, a diesel engine, a centrifugal fan, a plunger pump, a range extender, infrared laser sensors, a control box, and an operation monitoring module. The diesel engine (model: 192FA, rated power 8.2 kW, Changchai Co., Ltd.) was used for powering the plunger pump and the centrifugal fan (diameter 1.1 m, airflow volume 4.6 m^3/s, outlet air velocity 16 m/s, air pressure 0.6~0.8 MPa, rated speed 1500 rpm, Hongruiyuan Co., Ltd.). The range extender was a small gasoline engine (model: Dongwei-201, rated power 6 kW, Deleidun Co., Ltd.) for charging the battery pack during the operation. The main technical parameters of the spraying machine are listed in Table 1.

Principle of operation

To realize automatic target spraying, the target detection principle is the key (Cai *et al*., 2017; Jin *et al*., 2016). Compared with expensive ultrasonic and LiDAR sensors, infrared laser sensors have the advantages of long detection distance, low cost, *etc*., making them suitable for walnut orchards of large row spacing (Ricardo *et al*., 2011; Mitragotri 2023). Infrared laser sensors use the TOF (time of flight) principle for ranging. Each sensor has one signal emitter and one signal receiver. The sensor emits near-infrared light modulated waves, and when the waves reach the target, reflected waves are bounced back to enter the receiver. The distance between the sensor and the target can be calculated by Eq. 1.

$$D = \frac{c}{2} \cdot \frac{1}{2\pi f} \cdot \Delta t \qquad \text{(Eq. 1)}$$

where: D is the distance between the sensor and the target (m); c is the speed of light (3×10^8 m/s); f is the frequency of the sensor's near-infrared modulated waves (Hz); Δt is the time difference between waves emitted from the emitter and received by the receiver (s).

As shown in Figure 1, four infrared laser sensors were used on the designed spraying machine, two on the left side and two on the right. The sensors were mounted on steel poles, and their mounting heights could be adjusted to best fit the heights of the trees. The spraying nozzles were also divided into two groups. The opening/closing of each group was controlled by a solenoid valve. The longitudinal distance from the infrared laser sensors to the spraying nozzles was 0.84 m. This distance allowed enough time for the control system to respond to the real-time measurements of the infrared laser sensors and change the status of the nozzles accordingly.

Design of automatic target spraying system

Design of key components

Sprayer structure

The structure of the air-assisted sprayer needed to be designed according to the features of the walnut trees. The key structural parameters which influenced the performance of the spraying operation included the shape of the airflow channel, the number of nozzles and their installation angles, the height of the centrifugal fan, and the deflector angle.

Considering the wide row spacing and the shape of the walnut tree canopy, a circular airflow channel was designed for the centrifugal fan. Since each spray nozzle covered an angle of 30°, to make sure that the whole target area was covered, 10 nozzles were uniformly distributed along the airflow channel with an installation angle of 20° between two nozzles, as shown in Figure 2. Then, the spraying coverage effect of the nozzles was analyzed, and the mounting height of the centrifugal fan was determined. As shown in Figure 3, the spray from nozzles 5 and 6 was wasted, so these two nozzles were removed in the final configuration. Nozzles 1-4 and 7-10 were kept, and they were controlled as two separate groups.

When the air-assisted sprayer was in operation, the airflow distribution around the fan was a key factor influencing the movement of the liquid droplets. The airflow distribution was influenced by the installation angle of the deflector plates beside each nozzle. To investigate the effects of different installation angles of the deflector plates on the airflow distribution, a simulation model of the centrifugal fan was built in ANSYS FLUENT. Three angles were considered, 0°, 10° and 20°, as shown in Figure 4. The installation angle was defined as the intersection angle between the deflector plate and the line connecting the midpoint of the air outlet and the center of the fan.

The simulation procedures are as follows. A 3D model of the fan was first built in SolidWorks and then imported into FLUENT. Then a cubic flow field of a10-m side length was created using Workbench. Using triangular cells with sizes from 0.5 mm to 10 mm, meshing of the fan and the flow field was completed. In the simulation process, the K-epsilon turbulence model was chosen as the viscosity model. The air speed at the fan inlet was set to 25 m/s, and the outside natural wind speed was set to 1.5 m/s. Using the SIMPLE algorithm as the solver, the airflow around the fan was simulated. The velocity traces of the flow field outside the longitudinal section of the fan when the installation angle of the deflector plates was 0°, 10° and 20° are shown in Figure 5. From the results, the airflow coverage area was the biggest and the airflow distribution was the most uniform when the installation angle of the deflector plates was 10°. Thus, in the assembly process of the sprayer, the deflector plates were installed at 10°.

Arrangement of infrared laser sensors

As shown in Figure 1, four infrared laser sensors (model: TF-Luna, Benewake Co., Ltd.) were installed on the two steel poles of the spraying machine. The sensors were controlled as two groups. Since the shape of the walnut tree canopy was not always regular, using one single sensor for detection might result in misses of the canopy area and insufficient spraying. To make sure that the irregular canopy can be detected in time, on each side of the spraying machine, two laser sensors were installed as a group. The mounting height of the sensors could be adjusted from 1.7 m to 2.5 m. The guideline for height adjustment is as follows: when the walnut trees are young and the tree trunk is shorter than 1.5 m, the lower sensor should be mounted at 1.7 m and the upper sensor at 2.1 m maximum; as the trees grow, the mounting height of the upper sensor can be gradually raised from 2.1 to 2.5 m. As shown in Figure 6, the mounting heights of the two sensors were 1.7 m and 2.1 m, considering the top and bottom heights of the tree canopies. For tree 1 and tree 2, both sensors could detect the target at about the same time. However, for tree 3, sensor 1 missed the target when sensor 2 received a return signal. In the spraying control system, the nozzles were turned on when either sensor detected a target and were turned off when both sensors received no signal return. This control logic could ensure the best spraying effect, avoiding delayed opening and early closing of the nozzles.

Determination of airflow

The airflow volume of the centrifugal fan had a great impact on the spraying effect of the machine. A proper fan should be selected based on the required airflow volume and the air speed at the outlet. The determination of airflow volume should follow the principle of replacement (Zhang *et al.*, 2014), i.e., the air blown out from the fan needs to replace the air between the fan and the walnut trees on both sides. The airflow displacement schematic is shown in Figure 7. To enhance the spraying effect, the leaves of the walnut trees should be flipped by the airflow from the fan, and the determined airflow should be greater than the calculated displacement volume, i.e.

$$Q_W \geq V_1 K_1 L\left(H + h\right) \qquad \text{(Eq. 2)}$$

In Eq. 2, Q_W is the air volume of the fan (m^3/s); V_1 is the operating speed of the spraying machine (m/s); K_1 is the airflow attenuation and loss coefficient, generally 1.1-1.2; L is the distance from the sprayer to the tree trunk (m); H is the height of walnut tree canopy (m); h is the spraying width (m).

The minimum required airflow volume was calculated to be 4.28 m^3/s, and the following equation is satisfied:

$$Q_W = K_2 N F V_2 \qquad \text{(Eq. 3)}$$

In Eq. 3, K_2 is the airflow loss coefficient, generally 1.2; N is the number of air outlets; F is the area of air outlets (m^2); V_2 is the air velocity at the outlet (m/s).

After calculation, the minimum air velocity at the fan outlet was 12.6 m/s. Considering the necessary airflow reserve and possible leakage, an airflow volume of 4.6 m^3 and an air velocity at the outlet of 16 m/s were finally selected for the fan.

Hardware design of automatic target spraying control system

The main functions of the automatic target spraying control system included walnut tree detection and spraying nozzle control. The hardware of the control system mainly consisted of infrared laser sensors, solenoid valves, a microcontroller, electric relays, a DC battery pack, a voltage regulator, a speed sensor, a WIFI camera module, and a remote-control module. The hardware structure is shown in Figure 8. An Arduino UNO R3 microcontroller was used as the central control unit to interface with the sensors and execute the control program. The infrared laser sensors had a detection range of 0.2-8 m with an accuracy of 0.01 m. Two solenoid valves (model 2WH030-08B, AirTAC Group) were used to control the two groups of spraying nozzles. To monitor the operation status of the spraying machine and control its motion along the centerline of the tree row, a wireless camera module (model ESP-32CAM, 2 Mega pixels) was installed on the front of the machine. During the operation, the camera module transmitted the real-time images in front of the spraying machine through WIFI to a display terminal to assist the worker's control decision. An RPM sensor was used to measure the rotational frequency of the drive wheel of the tracked chassis to determine the operating speed of the spraying machine.

Program design of automatic target spraying control system

After the hardware design, a control program was designed for the automatic target spraying control system to realize acquiring and processing the information from the infrared laser sensors and controlling the opening and closing status of the solenoid valves. First, the microcontroller received data from the laser sensors. When any one from the two groups of laser sensors detected a target, the corresponding control port of the microcontroller would output a high-level voltage to turn on the solenoid valve. Otherwise, the solenoid valve was turned off when neither of the laser sensors detected a target. Meanwhile, the microcontroller calculated the real-time operating speed of the spraying machine according to the data returned by the RPM sensor and determined a time delay in opening and closing of the solenoid valve so as to improve the accuracy of the automatic target spraying control system. This speed-based delay time control was necessary for the spraying system to improve its accuracy (Sanchez and Zhang, 2023).

Since a distance of 0.84 m existed between the infrared laser sensors and the spraying nozzles, when the sensors detected a target, the nozzles were still behind the target.

The response time from the solenoid valves receiving the microcontroller's on/off control signals to the nozzles' opening/closing actions was very short. Thus, a proper time delay should be set in the control program to allow the nozzles to move to the right location, or the nozzles would always open and close earlier than required and the spraying accuracy was decreased. Since the distance between the infrared laser sensors and the spraying nozzles was constant and the response time of the solenoid valves and nozzles was relatively stable, the time lag was mainly influenced by the real-time operating speed of the spraying machine. In the control program, an operating speed-based time delay control strategy was designed, and the calculation equation is

$$T_1 = \frac{s}{v} - T_2 \quad \text{(Eq. 4)}$$

where: T_1 is time delay for the microcontroller to send solenoid valve control signals (s); s is the distance between the infrared laser sensors and the spraying nozzles (m); v is the real-time operating speed of the spraying machine (m/s); T_2 is the response time of the opening/closing of nozzles (m/s).

In Eq. 4, T_2 was experimentally determined. The consumed time from the moment when the microcontroller sends a control signal to the solenoid valve to the moment when the nozzles start or stop spraying was recorded. It was determined that the average nozzle opening time was 0.113 s and the average nozzle closing time was 0.173 s. Each time the microcontroller determined an on or off control signal for the solenoid valve, the real-time operating speed was obtained and T_1 was calculated. Then, the signal was sent to the solenoid valve after a delay of T_1.

Besides automatic spraying control, a manual control mode was added in the control program so that the spraying function could be controlled manually through the remote controller. The microcontroller used three digital ports A0, A1 and A2 to communicate with the three channels of the remote controller. When executing the control program, the microcontroller repeatedly checked the status of the three ports. The status of A2 determined the working mode of the spraying machine, high for manual and low for automatic. The A0 and A1 ports were responsible for the control of the left and right nozzles respectively. The designed program flowchart is shown in Figure 9.

Field experiments

Experimental plan

To evaluate the performance of the designed self-propelled target spraying machine, field experiments were performed in a standard walnut plantation in Yecheng County, Kashgar Region, Xinjiang in October 2023. Three groups of experiments were planned, including a comparison test of liquid consumption of continuous spraying and target spraying, a test of the amount of droplet deposition, and a test of the accuracy of automatic target spraying under different operating speeds. The walnut trees in the plantation were six years old in general. The experiments were carried out in sunny weather with an air temperature of 17 ℃ and air moisture of 22%. The natural wind speed was 0~2 m/s, direction southwest.

i) To verify the liquid saving effect of the target spraying machine, a comparison test between continuous spraying and target spraying was conducted. Three walnut trees in a row were selected as the test object. The total distance for spraying was 14.4 m, the gap between tree 1 and tree 2 was 1.55 m and between tree 2 and tree 3 was 0.65 m. The total length of the canopy gap was 2.20 m, a gap ratio of 15.3%. Three operating speeds, 0.4 m/s, 0.7 m/s, 1.0 m/s were used for the experiments. In each test, the total amount of liquid in the tank before and after spraying were recorded, and the difference was regarded as the consumed liquid. For each speed, three test were repeated and the average results were calculated.

ii) To test the spraying performance of the designed sprayer, a group of droplet deposition experiments were conducted. The trees for spraying were the same as the ones used in the previous test. The liquid used in this test were mixed with 0.1% lemon yellow solution, and seven sampling points were selected on the walnut trees, as shown in Figure 10. On each sampling point, two pieces of circular filter paper with a diameter of 7 cm were fixed on the front and back of one leaf. After spraying, the filter papers were left to dry and then brought to the laboratory for result analysis. The amount of droplet deposition on the filter paper was detected using a visible spectrophotometer (model 722S, Shanghai INESA Analytical Instrument).

iii) The third group of experiments aimed to test the spraying accuracy of the designed machine under different operating speeds. Three consecutive walnut trees were selected as the test object. The total distance for spraying was 15.96 m, the gap between tree 1 and tree 2 was 1.82 m, and the gap between tree 2 and tree 3 was 1.3 m. During the test, a white cloth of 18 m in length and 1.5 m in width was fixed to the opposite side of the target walnut trees. The control program was modified to allow the left group of nozzles to be turned on when the right-side infrared sensors detected a target. The experimental scene was shown in Figure 11. The white cloth was used to record the sprayed liquid, and the marks were measured and compared with the tree gaps and canopy lengths to determine the delayed or advanced distances. Three operating speeds, 0.4 m/s, 0.6 m/s and 0.7 m/s, were tested in the experiment. At the end of each test, the widths of the sprayed areas on the cloth were measured. The relative position difference between the left edge of the sprayed area on the cloth and the left edge of the tree canopy was deemed as the nozzle opening distance error, and the relative position difference between the right edge of the sprayed area on the cloth and the right edge of the tree canopy was deemed as the nozzle closing distance error. In each test, the nozzle opening and closing distance errors with respect to the three trees were averaged as the final results.

Results and Discussion

Comparison of continuous spraying and target spraying

When the operating speed of the spraying machine was 0.4 m/s, the average liquid consumptions/standard deviations under the continuous spraying mode and the target spraying mode were 3.209 L/0.091 L and 2.503 L/0.157 L respectively. The data were 1.861 L/0.083 L, 1.412 L/0.091 L for 0.7 m/s and 1.476 L/0.091 L, 1.091 L/0.120 L for 1.0 m/s. It can be calculated that compared with continuous spraying, target spraying could save a large amount of liquid. The liquid saving percentages under 0.4 m/s, 0.7 m/s and 1.0 m/s were 22.0%, 24.1% and 26.1% respectively, all greater than the gap ratio of the walnut trees, which was 15.3%. The reason was that the gap between walnut trees was measured from the maximum stretches of the tree canopies, and the two infrared sensors could not cover the whole profile of the canopy, which resulted in delayed opening and early closing of the nozzles. Meanwhile, as the operating speed increased, the liquid saving percentage also increased slightly, a phenomenon also seen in Jiang *et al*. (2016). This was due to the fact that the data returned from the sensors reduced at higher speeds and the detection accuracy was lowered. To achieve higher spraying accuracy, it was suggested that slow speeds should be used in practical spraying operations.

Droplet deposition

The droplet deposition effect was tested under three operating speeds, 0.4 m/s, 0.7 m/s, and 1.0 m/s, and two nozzle orifice diameters, 1.2 mm and 1.0 mm. Figure 12 shows the amount of liquid deposited on the front surface of the leaves at each sampling point. It is noticeable that the amount of liquid deposited on the sampling points under continuous spraying was greater than that under target spraying. It is because under continuous spraying, the overall spraying amount was larger and the liquid pressure in the pipes was more stable than under target spraying, which made more liquid droplets drift further. Under both spraying modes, the droplet deposition amounts at the front, left and right of the canopy were the highest compared with other locations, since these three points were the closest to the nozzles. This droplet deposition amount pattern was similar to the result in Li *et al*. (2023).

Under the same operating speed, the droplet deposition amounts at the front sampling point when the orifice diameter was 1.0 mm were much smaller than those when the orifice diameter was 1.2 mm. When the orifice diameter was reduced, the sprayed droplets became smaller and more pulverized, reducing their travelling speeds to reach further distances. When the operating speed increased, the droplet deposition amounts at all locations became smaller. For example, the deposition amounts at the front and bottom sampling points were reduced from 258 mg and 158 mg to 170 mg and 25 mg respectively after the speed was increased from 0.4 m/s to 1.0 m/s. The reason is that when the speed increased, the canopy disturbance period by the airflow was shorter and fewer droplets were deposited on the leaves. However, under all three speeds, the sprayed liquid was able to cover the whole canopy region, including the back sampling point. Figure 13 shows the droplet deposition amounts on the opposite surfaces of the sampling points under three operating speeds and two orifice diameters. Compared with Figure 12, the amounts were much lower than those on the front of the sampling points, which was reasonable since the liquid droplets could only deposit on the opposite of the leaves after the airflow from the fan turned the leaves around. Overall, under all six groups of speeds and orifice diameters, the designed target spraying machine could perform the required operation, and the droplet deposition amounts reduced as the machine's operating speed increased and the orifice diameter of the nozzles decreased. The growers should choose a proper operating speed and nozzle size considering requirements of both the spraying effect and efficiency.

Accuracy of automatic target spraying

The spraying accuracy of the automatic target spraying control system was tested at three different speeds. The average delay distances of nozzle opening and closing are shown in Table 2. It can be seen that when speed increased, the delay distance was kept stable, which indicates that the operating speed-based time delay control strategy was effective. From 0.4 m/s, 0.6 m/s to 0.7 m/s, the average delay distance for nozzle opening was 0.135 m, and the average delay distance for nozzle closing was 0.184 m. These values were comparable to the results in Dou *et al*. (2022), in which the delay distance for nozzle opening and closing of a LiDAR-based target spraying system were 0.122 m and 0.185 m respectively. Overall, the designed automatic target spraying control system could realize spraying distance errors of less than 0.2 m, meeting the requirements for walnut tree spraying operation. The delay distance for nozzle closing was slightly larger than that for nozzle opening. The reason is that when the solenoid valve was turned off under the microcontroller's output signal, the remaining liquid in the connecting pipe from the valve to the nozzles still had a spraying motion, which extended the spraying distances of the nozzles.

Conclusions

The following conclusions can be drawn from this work:

i) A self-propelled target spraying machine was designed, fabricated and tested for walnut tree plantations in Xinjiang. The tree canopy detection function was realized by low-cost infrared laser sensors. The structure, operation principle and key components of the automatic target spraying control system were introduced. To improve the spraying accuracy, an operating speed-based time delay control strategy was designed and implemented.

ii) Field experiments were performed to evaluate the performance of the designed spraying machine. The comparison test between continuous spraying and target spraying verified the effectiveness of liquid saving under different operating speeds. The droplet deposition test showed that the droplet deposition amounts at all seven sampling points reduced as the machine's operating speed increased and the orifice diameter of the nozzles decreased. However, the sprayed liquid was able to cover the whole canopy region of the walnut trees under all speed and orifice diameter combinations.

iii) The test of the automatic target spraying accuracy showed that the designed operating speed-based time delay control strategy was effective. The designed target spraying machine and its corresponding automatic control system could meet the accuracy requirements for practical spraying operations in walnut orchards in Xinjiang.

References

Berk, P., Hocevar, M., Stajnko, D., Belsak, A. 2016. Development of alternative plant protection product application techniques in orchards, based on measurement sensing systems: A review. Comput. Electron. Agr. 124:273-288.

Cai, J., Wang X., Song, J., Wang, S., Yang, S., Zhao, C. 2017. Development of real-time laser-scanning system to detect tree canopy characteristics for variable-rate pesticide application. Int. J. Agr. Biol. Engin. 10:155-163.

Chen, Z., Chen, J., Song, S., Sun, D. 2022. Development and experiments of the hanging flexible targeted spray device for orchards. T. CSAE 38:11-20.

Chen, Z., Hu, Z., Xiong, Y., Wang, P., Yu, Y., Peng, M. 2023. Design and test of the canopy wrap-around profiling-to-target sprayer for orchards. T. CSAE 39:23-32.

Chi, M., Song, J., Zeng, A., Liu, Y., Song, W., Zhang, L. et al. 2010. Effect of spraying conditions on dermal exposures. T. CSAE 26:276-282.

Deng, W., He, X., Zhang, L., Zeng, A., Song, J., Zou, J. 2008. Target infrared detection in target spray. Spectrosc. Spect. Anal. 2008:2285-2289.

Dou, H., Zhai, C., Wang, X., Zou, W., Li, Q., Chen, L. 2022. Design and experiment

of the orchard target variable spraying control system based on LiDAR. T. CSAE 38:11-21.
Gil, E., Llorens, J., Llop, J., Fàbregas, X., Escolà, A., Rosell-Polo, J.R. 2013. Variable rate sprayer. Part 2 – Vineyard prototype: Design, implementation, and validation. Comput. Electron. Agr. 2013; 95: 136-150.
Gu, C., Wang, X., Wang, X., Yang, F., Zhai, C. 2022. Research progress on variable-rate spraying technology in orchards. Appl. Eng. Agr. 36:927-942.
Huang, Z. 2020. Research on variable-rate spray control system of crawler-type orchard sprayer. PhD Thesis, Jiangsu University.
Jiang, H., Bai, P., Liu, L., Dong, X., Song, J., Zhang, X. 2016. Caterpillar self-propelled and air-assisted orchard sprayer with automatic target spray system. T. CSAM 47:s189-195.
Jin, X., Dong, X., Yang, X., Yan, H. 2016. Design and experiment of target spraying system of 3WGZ-500 sprayer. T. CSAM 47:21-27.
Li, L., He, X., Song, J., Liu, Y., Zeng, A., Liu, Y. 2018. Design and experiment of variable rate orchard sprayer based on laser scanning sensor. Int. J. Agr. Biol. Engin. 11:101-108.
Li, W., Jiang, S., Xu, P., Ma, H., Yang, S., Zheng, Y. 2023. Design and experiment of self-propelled small target following sprayer for hilly orchard. T. CSAM 54:188-197.
Liu, H., Gao, B., Shen, Y., Hussain, F., Addis, D., Pan, C.K. 2018. Comparison of Sick and Hokuyo UTM-30LX laser sensors in canopy detection for variable-rate sprayer. Inf. Process. Agric. 5:504-515.
Mahmud, M., Zahid, A., He, L., Choi, D., Krawczyk, G., Zhu, H. 2021. Development of a LiDAR-guided section-based tree canopy density measurement system for precision spray applications. Comput. Electron. Agc. 182:106053.
Mitragotri, S. 2013. Sensors enabling precision spraying in agriculture: a case study. Proc. 16th Int. Conf. Sensing Technology (ICST), Hyderabad. pp. 1-6.
National Forestry and Grassland Administration. 2022. China forestry and grassland statistical yearbook. China Forestry Publishing House.
Ricardo, S., Jordi, L., Alexander, E. 2011. Innovative LIDAR 3D dynamic measurement system to estimate fruit-tree leaf area. Sensors (Basel) 1: 5769-5791.
Sanchez, P.R., Zhang, H. 2023. Precision spraying using variable time delays and vision-based velocity estimation. Smart Agr. Technol. 5:100253.
Wei, Z., Xue, X., Salcero, R., Zhang, Z., Gil, E., Sun, Y. 2022. Key technologies for an orchard variable-rate sprayer: Current status and future prospects. Agronomy 13:59.
Yan, C., Xu, L., Yuan, Q., Ma, S., Niu, C., Zhao, S. 2021. Design and experiment of vineyard variable spraying control system based on binocular vision. T. CSAE 37:13-22.
Zhai, C., Zhao, C., Wang, N., Long, J., Wang, X., Zhang, H. 2018. Research progress on precision control methods of air-assisted spraying in orchards. T. CSAE 34:1-15.
Zhang, X., Jiang, Z., Fan, G., Cao, L. 2014. Self-propelled crawler directional air-blowing orchard sprayer. T. CSAM 45:117-122.
Zheng, Y., Chen, B., Lyu, H., Kang, F., Jiang, S. 2020. Research progress of orchard plant protection mechanization technology and equipment in China. T. CSAE

36:110-124.
Zheng, Y., Jiang, S., Chen, B., Lyu, H., Wan, C., Kang, F. 2020. Review on technology and equipment of mechanization in hilly orchard. T. CSAM 51:1-20.

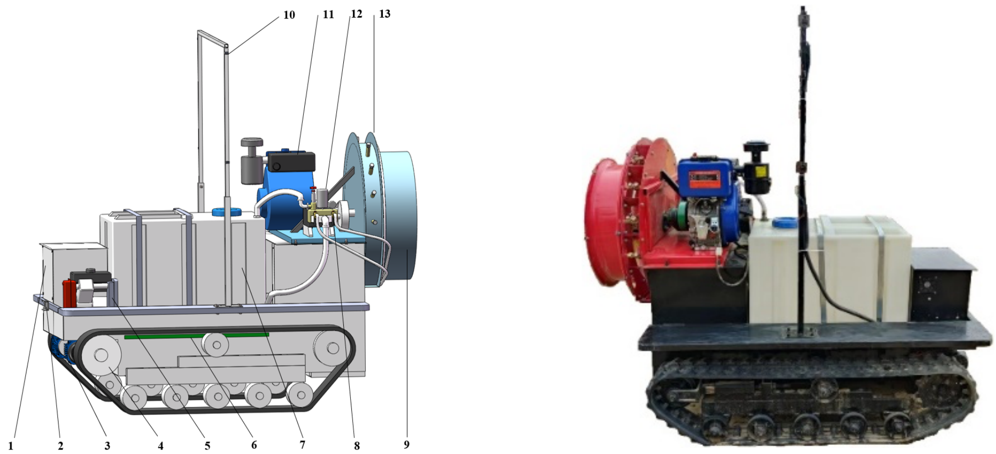

(a) Schematic diagram (b) Prototype

Figure 1. Self-propelled target spraying machine. 1. Control box, 2. Operation monitoring module, 3. Brushless DC motors, 4. Tracked chassis, 5. Range extender, 6. Battery pack, 7. Sprayer tank, 8. Solenoid control valve, 9. Centrifugal fan 10. Infrared laser sensors, 11. Diesel engine, 12. Plunger pump, 13. High pressure nozzles

Table 1. Main technical parameters of the spraying machine.

Parameters	Value
Overall dimension /mm	2000×1300×1500
Overall mass /kg	400
Speed range /m·s^{-1}	0-1.5
Spraying width /m	7
Spraying height /m	7
Number of nozzles	8
Chassis ground clearance /mm	200
Track width /mm	180
Motor power /kw	1.8
Tank capacity /L	300
Battery capacity /Ah	52
Rated diesel engine power /kw	8

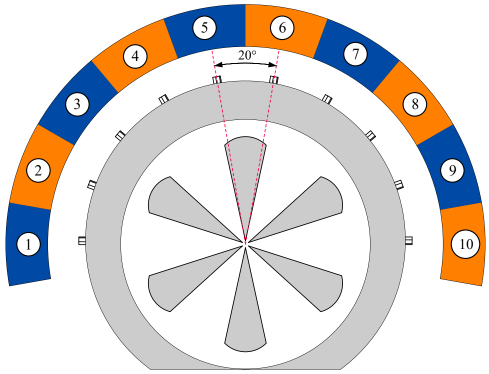

Figure 2. Schematic of nozzle arrangement.

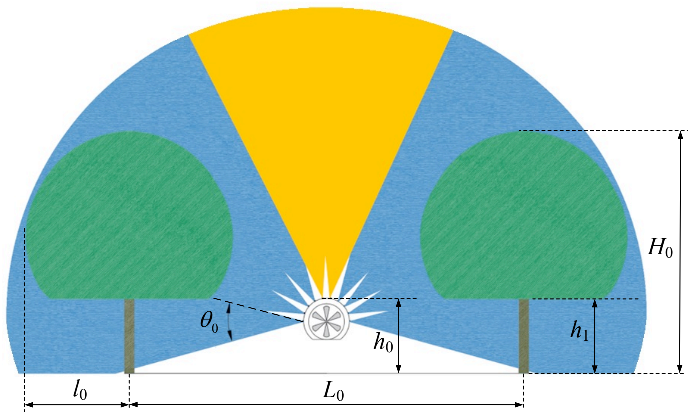

Figure 3. Schematic of nozzle spraying coverage. L_0=8.0 m is the row spacing, l_0=2.0 m is half of the canopy thickness, h_0=1.6 m is the distance from the top of the centrifugal fan to the ground, h_1=1.5 m is the average height of the tree trunk, H_0=5.0 m is the average tree height, and θ_0=30° is the coverage angle of each nozzle.

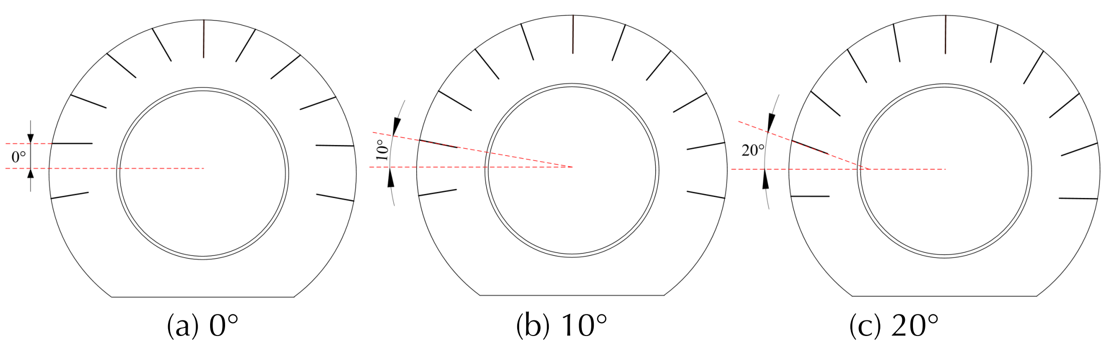

Figure 4. Schematic of different installation angles of deflector plates.

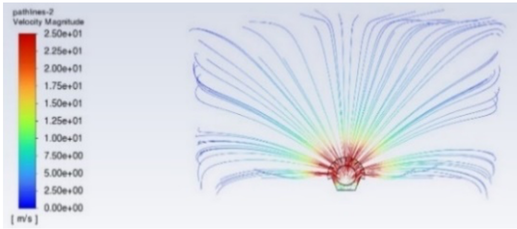

(a) deflector plate angle = 0°

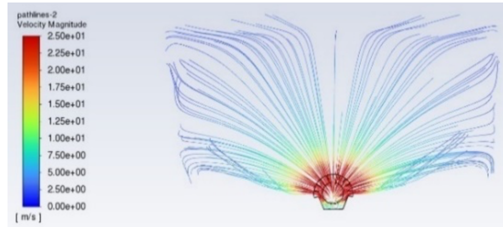

(b) deflector plate angle = 10°

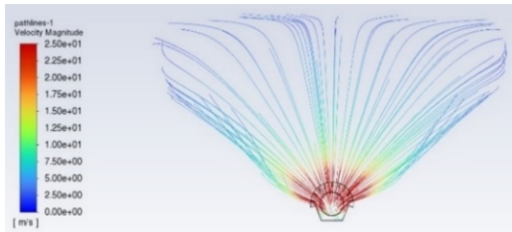

(c) deflector plate angle = 20°

Figure 5. Velocity traces of the flow field outside the longitudinal section of the fan.

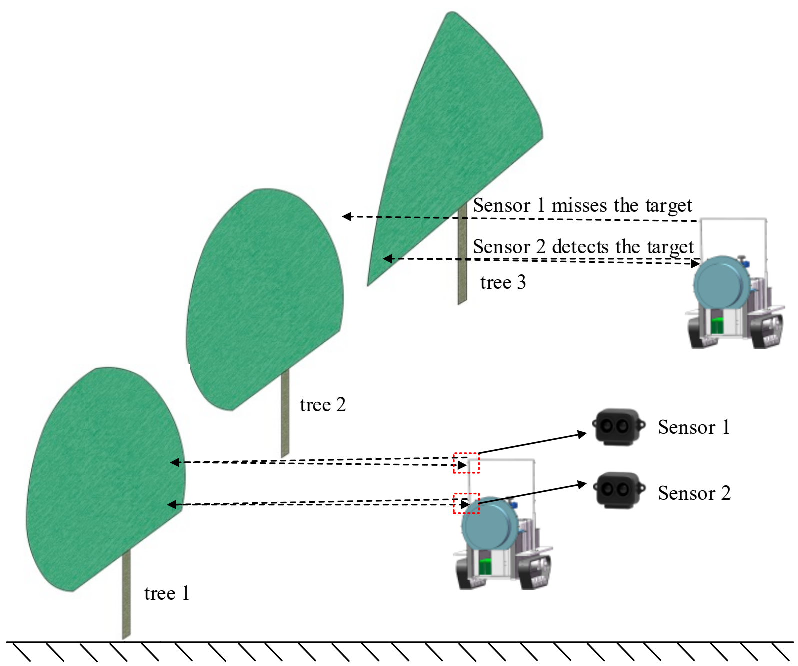

Figure 6. Schematic of infrared laser sensor arrangement.

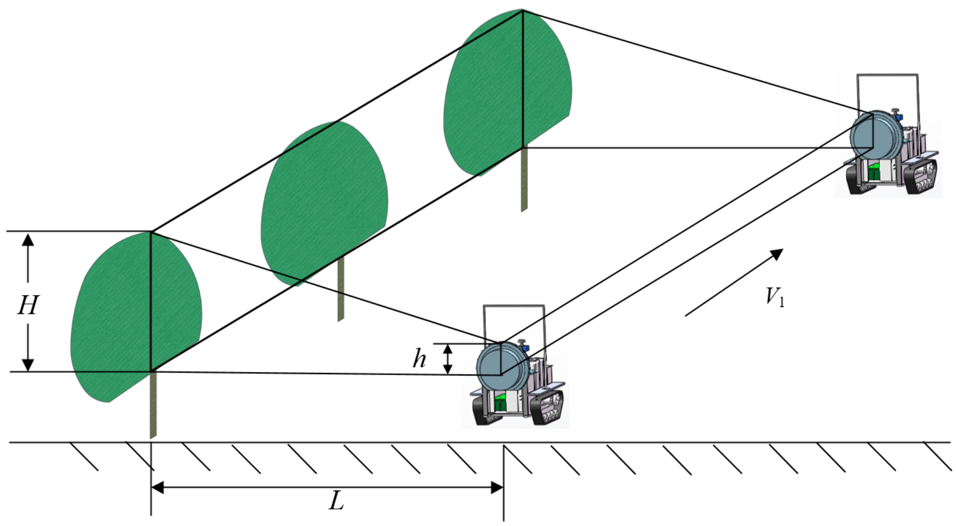

Figure 7. Schematic of air displacement principle.

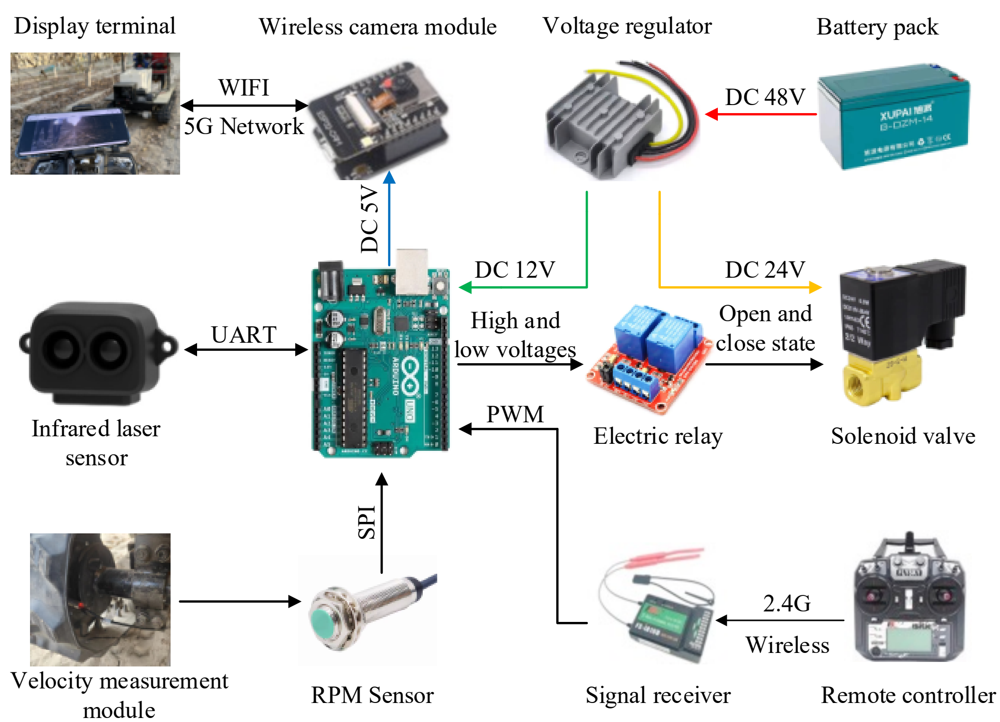

Figure 8. Hardware structure of the automatic target spraying control system.

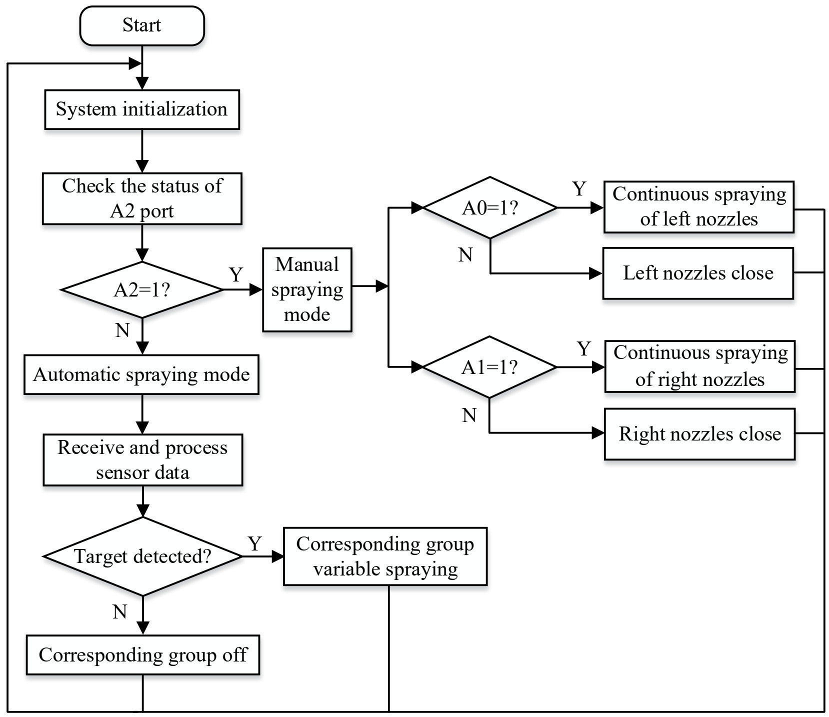

Figure 9. Control program flowchart.

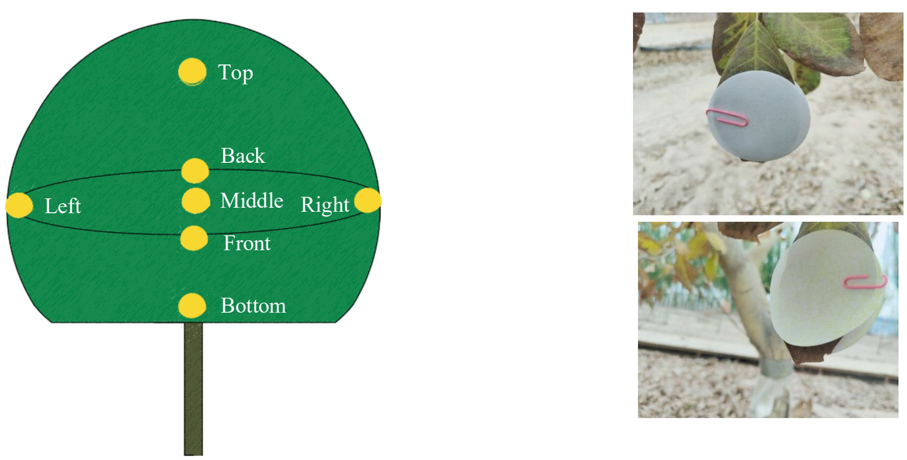

(a) Schematic b) Filter papers before and after spraying

Figure 10. Arrangement of sampling points on walnut trees.

Figure 11. Experimental scene of spraying accuracy test.

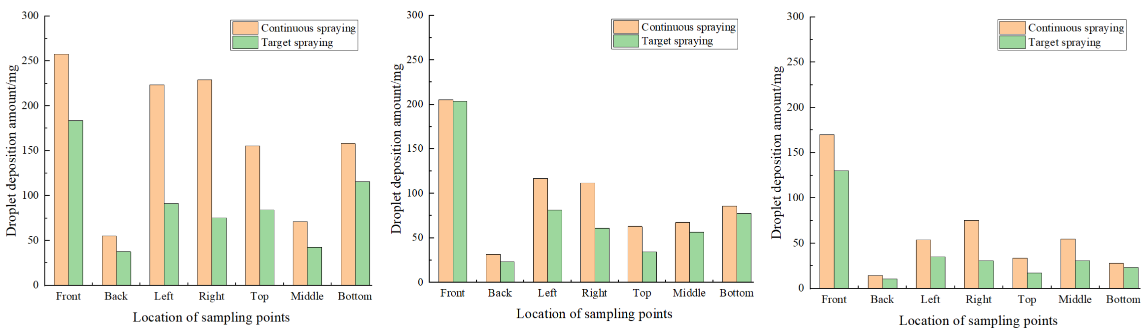

(a) 0.4 m/s, 1.2 mm (b) 0.7 m/s, 1.2 mm (c) 1.0
m/s, 1.2 mm

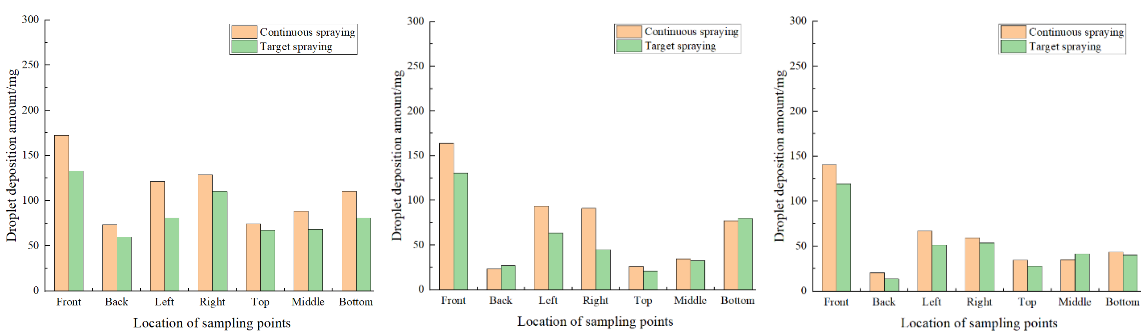

(d) 0.4 m/s, 1.0 mm (e) 0.7 m/s, 1.0 mm (f) 1.0 m/s,
1.0 mm

Figure 12. Droplet deposition amounts on the front surfaces at seven sampling points.

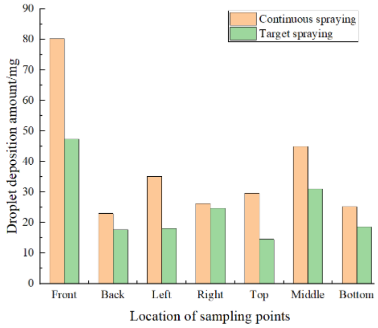

(a) 0.4 m/s, 1.2 mm

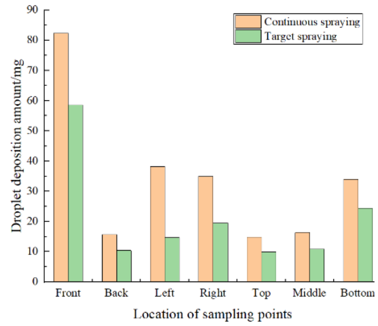

(b) 0.7 m/s, 1.2 mm

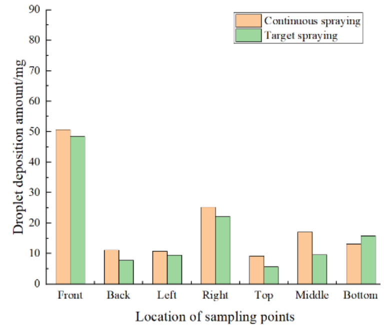

(c) 1.0 m/s, 1.2 mm

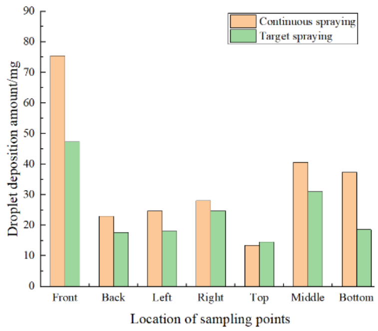

(d) 0.4 m/s, 1.0 mm

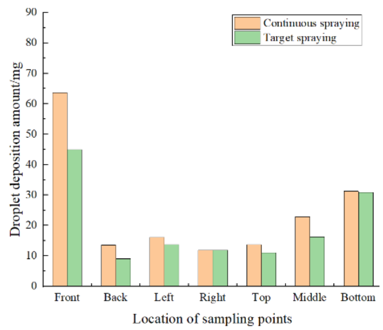

(e) 0.7 m/s, 1.0 mm

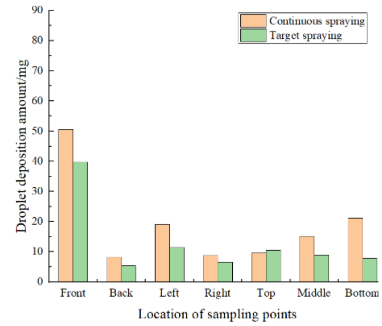

(f) 1.0 m/s, 1.0 mm

Figure 13. Droplet deposition amounts on the opposite surfaces at seven sampling points.

Table 2. Results of target spraying accuracy test.

Nozzle status	Operating speed/m·s^{-1}	Average delay distance /m
Opening	0.4	0.131
	0.6	0.138
	0.7	0.136
Closing	0.4	0.179
	0.6	0.185
	0.7	0.187